Kasetsart J. (Nat. Sci.) 37 : 209 - 218 (2003)

Properties of Titanium Nitride Film Coated on Stainless Steel 304

Nitinai Udomkan[1],**Vilasinee Sutorn**[2], **Pichet Limsuwan**[1] **and Pongtip Winotai**[3]

ABSTRACT

The characteristics of titanium nitride (TiN) film coated on the stainless steel substrates were studied under various processing conditions, e.g., different nitrogen flow rates and substrate temperatures. The TiN film was produced by reactive magnetron sputtering process under mixed gases pressure of argon and nitrogen with the stainless steel 304 substrates. X-ray diffraction was used to verify the TiN crystalline structure. The diffraction patterns of Ti_2N(101)and TiN (111)phase at 2θ =34.50° and 36.10°, respectively,were found when the nitrogen flow rate was 3.338 sccm.The nitrogen flow rates of 3.84 and 7.80 sccm only the TiN (111) peak was observed at 2θ = 36.10°. Scanning electron microscopy examination indicated that the film structure was more uniform and denser for higher substrate temperature. At 250°C, the film structure was nonuniform, there were some grooves and a big hump on titanium nitride film. Hardness measurements were performed by Nano Inderter to determine the mechanical properties of the films. A color of film was measured by spectrophotometer. TiN films have a uniform golden color. The result showed that the surface hardness of stainless steel which was coated with this film was higher. The film hardness at 50 nanometer depth was higher than that at 100 nanometer for films thickness of about 1 micron. The experiment result showed the highest hardness was obtained when nitrogen flow rate was 7.80 sccm and titanium nitride film was TiN-phase.

Key words: reactive magnetron sputtering;titanium nitride;nano-hardness

INTRODUCTION

Owing to its superior mechanical properties, titanium nitride (TiN) films are widely utilized in many industrial areas where high abrasion resistance, low friction coefficient, high temperature stability, and high hardness are required. The mechanical properties of TiN are strongly related to its preferred orientation (Chou,2002;Huang,2002).It has been reported that TiN film with (111) preferred orientation possesses the highest hardness. During the Physical Vapor Deposition (PVD) of a thin film, the packing density and preferred orientation of the film normally change with the increasing film thickness. Therefore, film thickness is an important parameter that affects the preferred orientation and hardness of the coating. Among the transition metal nitride, owing to its superior properties and well-established coating technology, TiN coating is usually chosen as the protective film for many metals to prolong their service life. One of major applications for the protection purpose is the coating on stainless steel. By coating TiN film, both corrosion resistance and

1 Department of Physics, Faculty of Science, King Mongkut's University of Technology Thonburi, Prachautid Road, Bangkok 10140,Thailand.

2 National Science and Technology Development Agency, 114 Paholyothin Rd., Pathumthani 12120 Thailand.

3 Department of Chemistry, Faculty of Science ,Mahidol University,Rama 4th Rd., Bangkok 10400,Thailand.

Received date : 21/04/03 Accepted date : 30/06/03

surface hardness of stainless steel is increased, and golden decorative colors add the product value as well.

Surface treatments like coating can dramatically enhance the surface mechanical properties of steel components and make the control of wear and friction possible over a wide rang of tribological condition (Badisch, 2003). This work reports the scanning electron microscopy (SEM) / X-ray diffraction and Raman scattering studies of such solid lubricant coating .The Raman spectra are collected using a recently developed near infrared Raman spectroscopy (Karim, 2002). Coating, specifically physical vapor deposition (PVD) coatings such as titanium aluminum nitride (TiAlN), titanium nitride (TiN), titanium carbonitride (TiCN), and chromium nitride (CrN), provide coating that are harder than the substrate on which they are deposited (Matsuda, 1998). Titanium nitride (TiNx) thin films are widely used as wear-resistant coating for tools and wear parts and surface decoration for commercial goods.Recently, they have been used in semiconductor devices. A number of techniques are currently available for the deposition of TiN films;TiN films prepared by reactive sputtering can be used as wear-resistant coatings and diffusion barriers in the metallization technology of Si devices. Surface treatment like such coating can dramatically enhance the surface mechanical properties of steel components and make the control of wear and friction possible over a wide range of tribological condition (Chire, 2003). This work is the first report of combined tribological, scanning electron microscopy (SEM), X –ray diffraction (XRD), Raman Microscopy, CIE L*a*b* color Index and Nano Indenter imaging studies of such solid lubricant coatings, specifically physical vapor deposition (PVD) coatings such as titanium nitride (TiN) on Stainless Steel 304.The aim of this study is to investigate the effect of film thickness on the structure and mechanical properties of TiN coating on stainless steel 304.

MATERIALS AND METHODS

The substrate material used in this study was 304 stainless steel with a composition of 0.1%Cu, 0.14%Co, 0.44%Si, 1.18%Mn, 8.73%Ni, 18.57%Cr, and the balance being Fe. Prior to the coating process, the specimens underwent ultrasonic cleaning progressively in acetone and ethanol and then dried in a vacuum dryer. The coating process was carried out in an EDWARD VACUUM E306 sputtering system. The schematic diagram of the system is shown in Figure1. Before deposition the substrates were gradually heated to a temperature of 300°C, 350°C, 370°C. Meanwhile, the coating chamber was evacuated to 8.0×10^{-4} Pa to avoid the contamination process. Prior to deposition, the substrate surface was sputtered cleaned by Ar ions for 10 min at a pressure of 10 Pa Ar and –840 V substrate negative dc bias voltage.The evaporation of the Ti source by the electron beam was initiated by introducing 1.8×10^{-3} mbar of Ar and maintaining the gun power at 6 kW.A negative dc bias voltage of -840 V was applied to the substrate (Matsuda,1998).The coating conditions of all samples were the same except that the deposition duration were varied to control the film thickness.The crystal structure of the TiN films was identified by X–ray diffraction (XRD). The Cu Kα was used as the source for diffraction. The XRD analysis was focused on the determination of (111) preferred orientation and residual stress.The extent of (111) preferred orientation is quantified by a texture coefficient = I(111)/[I(111)+I(200)], where I is the integrated intensity of the corresponding Bragg peak. The thickness of each TiN film and the composition depth profile were measured by Raman spectrometer model E-2000, Renishaw. The change in color (CIE L*a*b* color index) of the chosen coated surface was monitored by the imaging spectrophotometer (LambdaSpec Instruments) by allowing light rays perpendicular to the surface. Since large substrate effect may

occur in the TiN films coated on 304 stainless steel when using normal microhardness, the hardness was measured using a Nanoindenter. To evaluate the creep effect, the load pattern was first increased linearly from 0 to the maximum load in 5 s, staying at the maximum load for 5 s and then releasing the load linearly from the maximum load to 0 in 5 s. For each sample, five measurements were performed and the average value was reported.

RESULTS AND DISCUSSION

Raman signal from the TiN layers

All the properties of the sample vary systematically with their preparation conditions. The Raman signals are highly reproducible. The Raman contributions from the different layers of a sample are cumulative. Therefore, the Raman spectrum will be obtained by subtracting the TiN contribution to this Raman spectrum from the whole Raman signal of the sample. The micro Raman spectra were recorded at room temperature. They were excited at energies Eex of 2.71 eV (514 nm) by Ar lasers. Figure 2 shown the Raman spectra of the samples excited by the 514-nm laser light. All spectra have the same square-like shape at 190- 350 cm^{-1} and a triangular-like shape at approximately 810 and 1110 cm^{-1}. The same structures are found in thin films and crystal of cubic rocksalt TiN (Chire, 2003, Richter, 1996). The square-and triangular- like signals are defect-induced first-order Raman scattering, because, like thicker TiN films and TiN crystal, these 4.5 nm TiN film contain Ti and N vacancies. The square – like signals with TA and LA modes, originate from Ti atoms surrounding N vacancies and N atoms surrounding Ti vacancies, respectively (Richer, 1996, Mcneil, 1993). The small 414 cm^{-1} (2TA) structure and the wide maxima around 810(LA+TA) and 1110(2TO) cm^{-1} originate from

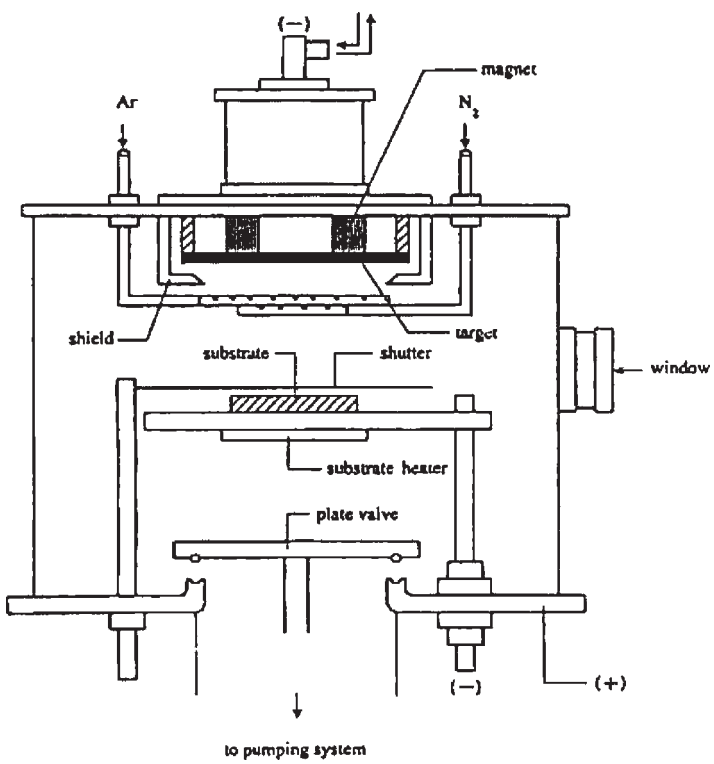

Figure 1 Schematic cross-sectional view of magnetron sputtering chamber.

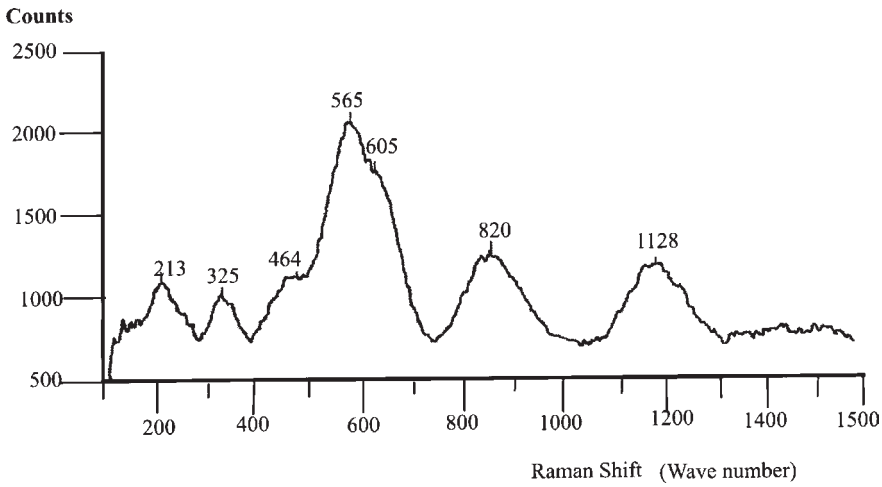

Figure 2 The Raman spectrum of the sample.

the overtones. Some characteristics of the TiN layers in nm-size TiN (5.0 nm) superlattices were derived from Raman measurements.In particular,in this thickness range,the chemical composition of the TiN layers depends on the thickness layers. Actually, as in all other known rocksalt TiN materials, our TiN layers contain both N and Ti vacancies, with an overall N sub-stoichiometry TiN_{1-X} in superlattices x = 2-3%. This is ascribed to N diffusion standing in the vicinity of the TiN interfaces to the TiN layers. It could possibly be ascribed to a defect-induced first-order Raman signal from a defective rocksalt cubic phase of TiN interfaces.

Layer analysis by Nano – Indentor method

The hardness of the TiN film coated on 304 stainless steel was measured using a nanoindenter. Considering the indentation size effect, the load of the indenter was chosen to limit the penetration depth less than one tenth of the film thickness in order to minimize the effect of substrate on hardness of the thin film. Figure 3 shows the variation of the hardness with the film thickness.The nanohardness values are ranging from 6.75 to 24.1 G Pa.(Badisch, 2003; Karim, 2002). To confirm the hardness, mostly a quartz standard sample was used to calibrate the nanoindenter, and the accuracy of the hardness was within 5%. In addition, five indentations were made and the average value was reported. The precision of each value is within 10% from Figure 5 and 6, a general trend is observed that the hardness of TiN increased with the film thickness. The hardness rapidly increased as thickness varied from 50 nm to 100 nm and saturated to a value of approximately 24.1 G Pa.

Structure and Layer analysis by XRD

Figure 7 shows the XRD diffraction patterns of all the TiN coated samples, with 2θ scanning from 30° to 50°. Despite the known atomic structure of compounds in the Ti-N system, the properties of thin films made from these materials depend strongly on their real structure. X –ray diffraction (XRD) analysis can also give information about some microstructure aspects of thin films,e.g. size of coherently diffracting blocks or preferred orientation of grains. However, XRD also gives information on phase composition, lattic parameter, residual stresses and microstrains in thin film,which are structure features with small differences of the order of a few picometers in individual films. These structural aspects of thin films can thus be regarded as their picostructure. It is mainly these

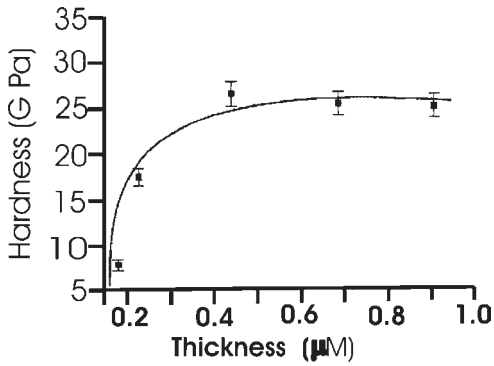

Figure 3 Nitrogen flow (ϕN) and microhardness.

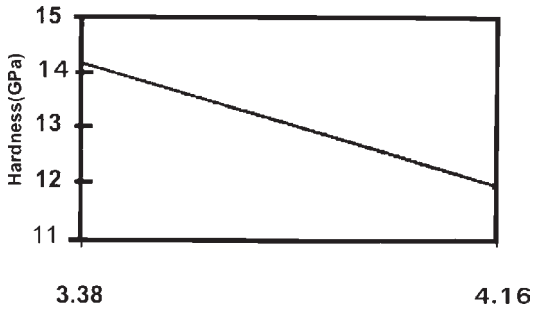

Figure 4 Microhardness distribution with nitrogen florate.

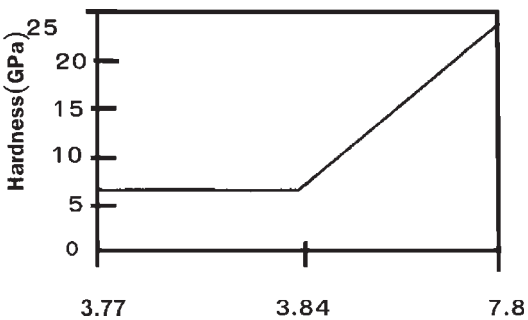

Figure 5 Hardness and nitrogen flow rate.

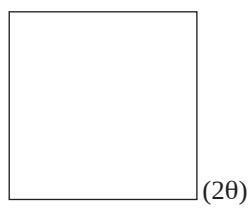

Figure 6 Selected X-ray diffraction patters of TiN coating from ϕN = 3.84 sccm.

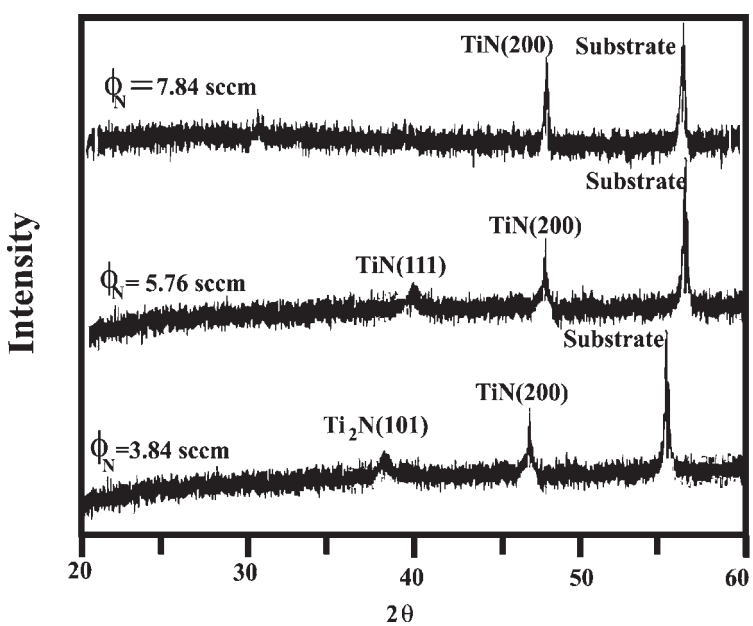

Figure 7 Selected X-ray diffraction patters of TiN coating.

picostructural aspects that will be summarized in the following sections.The effect of nitrogen content in Ti-N films is shown Figure 8. With increasing nitrogen content the structure of the films changes from a hexagonal solid solution of nitrogen in α - Ti to the cubic δ phase of TiN. In some cases the tetragonal interphase Ti_2N was observed during the transition from α - Ti solid solutions to δ- TiN compounds, however, the hardest films contain no Ti_2N phase but only the cubic TiN phase. Figure 8 shows selected parts of the X-ray diffraction patterns for stoichiometric TiN and for the film consisting of Ti_yN_x phase. Figure 7 shows that, for ϕ_N = 3.84 sccm, only strong TiN_x(111) and weak TiNx (200) peaks are recorded at 2q = 36.20° and 42.50° respectively, revealing the formation of the f.c.c TiN_x compound only, for ϕ_N = 3.38 sccm, the peaks of Ti_2N(101) and Ti_2N (111) at 2θ = 34.80° and 39.50° respectively and a peak at 2θ = 37.30° are recorded. For ϕ_N = 3.38 sccm, the film cannot absorb all the N_2 offered, and part of the remaining N_2 reacts with the Ti target surface. Since the magnetic field is more intense close to the centre of the target, by

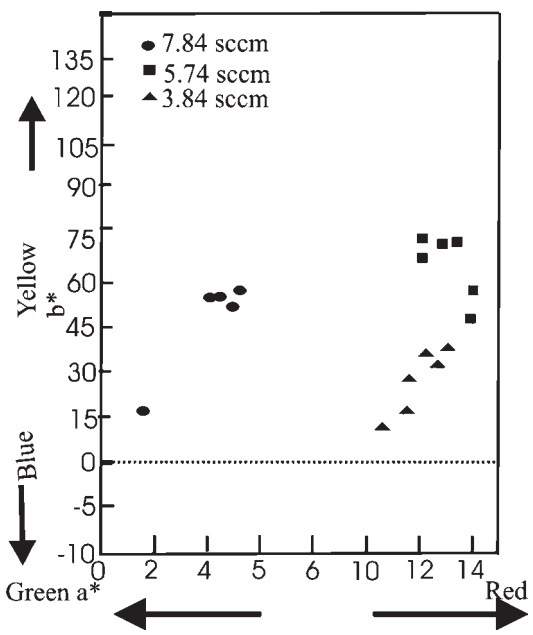

Figure 8 Color of TiN film coated stainless steel.

increasing ϕ_N the target surface is covered stepwise by the TiN_x compound from the perimeter to the centre (Chou,2002). Consequently, both Ti and TiN_x are sputtered from the target surface. However, since the sputtering rate of TiN_x is much lower than that of Ti, the deposition rate is expected to decrease with ϕ_N (Harma,1999; Hohl,1992; Hoffman, 1988). The diffraction patterns showed the formation of δ - TiN structure in the case of TiN. For the TiN we have found only the formation of the α solid solution. The δ -TiN structure is of NaCl type, compose of two f.c.c. sublattices, one containing the titanium atoms and the other the nitrogen atoms. In case of substoichiometric TiN_x samples, as we have here, it is known that vacancies take place on the nitrogen sublattice. The sample with α solid solution is not discussed here because its structure is of hexagonal types. The concentration scale studied here converse the definition range of δ -TiN_x (0.4 ≤1).

Layer analysis of TiN film by CIE L*a*b* color index

The change in color (CIE L*a*b* color index) of the chosen TiN film was monitored by the Perkin- Elmer reflectance spectrometer (Lambda 16) by allowing light rays incident surface of TiN film. The spectrometer was warmed up for at last 30 minutes and calibrated with $BaSO_4$. The color of TiN film was measured in visible region, i.e., from 400 nm to 700 nm. The color shown in Figure 9. We have investigated the influence of growth temperature at the successive operating points on the composition of the films obtained, and on their structure. Furthermore, we can note that whatever the point considered, the decrease of the N/Ti ratio, on increasing the temperature (T) to above the " critical temperature" , is accompanied by a radical change in the aspect of the coated surface. Indeed, the film surface which, before the sudden decrease in the N/Ti ratio had the right "traditional" gold yellow aspect of titanium nitride, then presents a matt yellow color. Fig 9. The

change in color of titanium nitride(Chire, 2003).

Structure of TiN films layer

The SEM observations for the two wear tracks shown in Figure 10 are confirmed Raman spectra analyses. This is also confirmed by the SEM/EDX image of an untested dry TiN surface shown in Figure 10. Which shows only the presence of TiN. Scanning electron microscopy (SEM) and Atomic Force Microscopy (AFM) examination indicated that the film structures were more uniform and denser for higher substrate temperature. At 350 and 450°C, (Richter, 1996) there were nonuniform film structures with some grooves and a big hump of titanium nitride film (Karin, 2002; Valvoda,1996). Figure5 showed surface roughness of film TiN coated on stainless steel substrates studied under SEM and AFM, with various processing condition e.g. different flow rates and substrate temperatures. Figure 10 and 11 showed the characteristics of surface titanium nitride (TiN) at SEM and AFM.

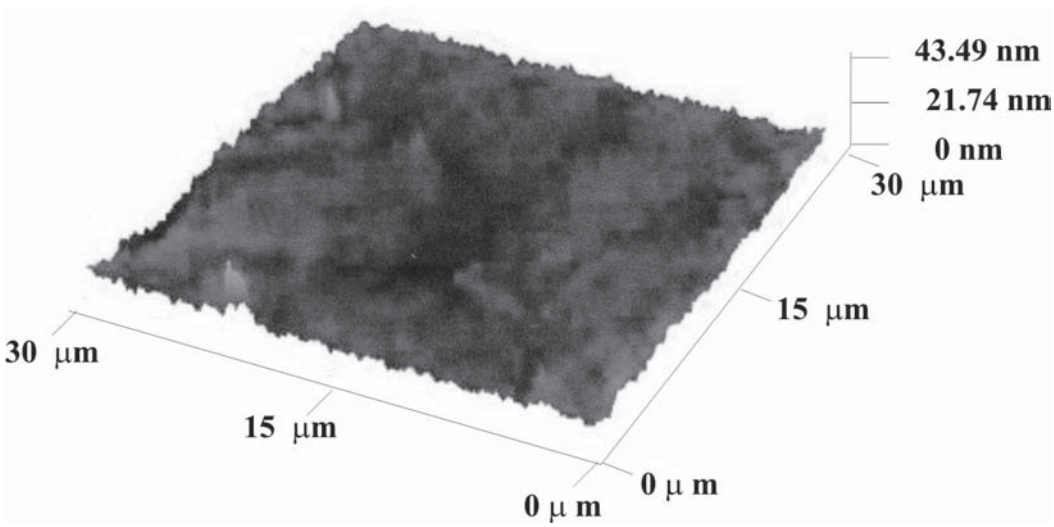

Figure 9 AFM of TiN film depostied at 3.84 sccm (nitrogen flow rate).

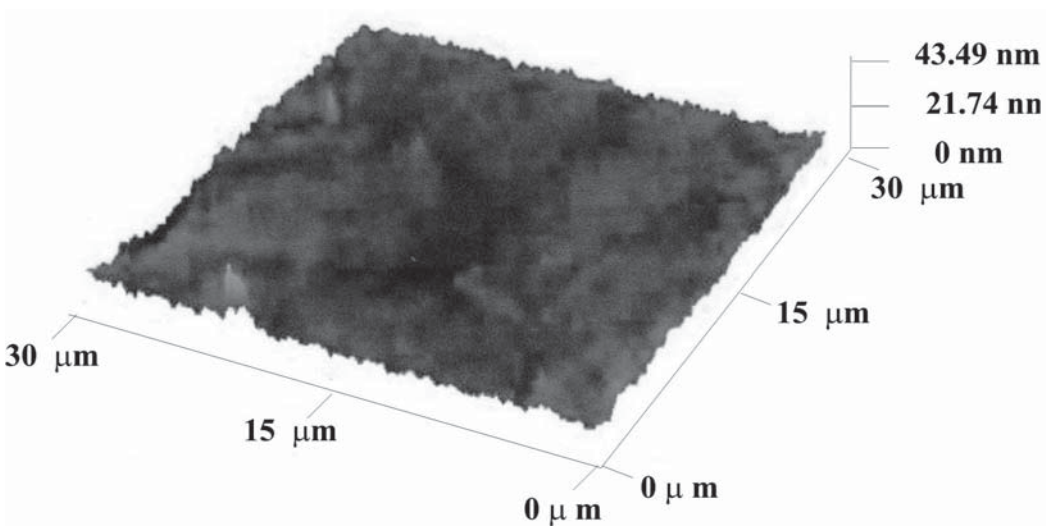

Figure 10 AFM of TiN film depostied at 5.76 sccm (nitrogen flow rate).

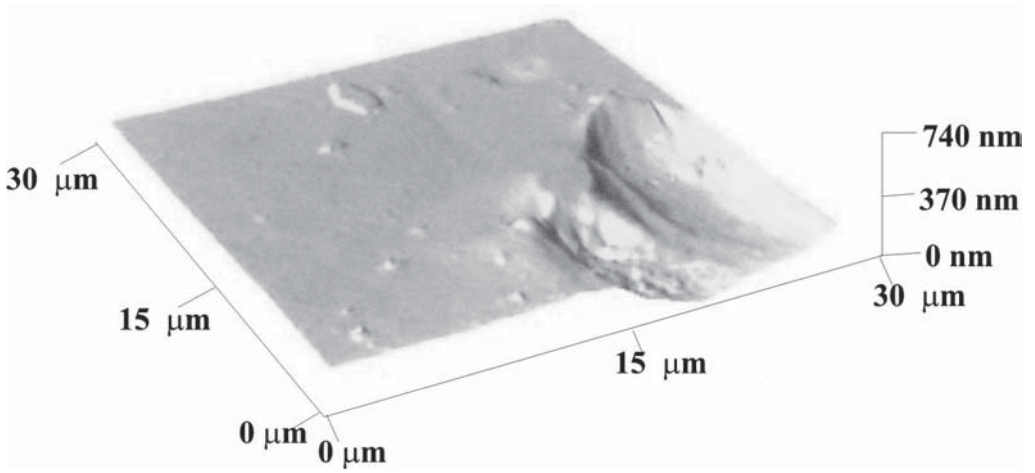

Figure 11 AFM of TiN film depostied at 7.84 sccm (nitrogen flow rate).

CONCLUSIONS

The hardness of the TiN film coated on 304 stainless steel was measured using a nanoindenter. Considering the indentation size effect, the load of the indenter was chosen to limit the penetration depth to be less than one tenth of the film thickness in order to minimize the effect of substrate on hardness of the thin film. The nanohardness values are ranging from 6.75 to 24.1 G Pa. The hardness values of the samples are all above 24 G Pa, which seems to be very high for TiN coatings compared with previously reported data, mostly less than 25 G Pa. Form Figure 6, a general trend is observed that the hardness of TiN increases with the film thickness. The hardness rapidly increased as thickness varied from 50 nm to 100 nm and saturated to a value of approximately 24 G Pa.The XRD diffraction patterns of all the TiN coated samples, with 2θ scanning from 30° and 50°. The TiN (111) preferred orientation obviously increases and the corresponding (111)g-Fe peak of the stainless steel decreases with increasing film thickness. Figure 7 shows the variation of the film hardness with the texture coefficient. The hardness increases as the (111) texture coefficient increases, especially as the texture coefficient above 0.5, the hardness rapidly increases to a saturated. From the experimental result, it is found that the hardness of TiN films change with a few factors; namely, the film thickness, the texture coefficient and the packing factor. Comparing Figure 6 and Figure 7, one can find that these three figures all have the similar trend that hardness increase with the creasing factors such as film thickness, (111) texture coefficient or packing factor. From Figure6 the hardness increases from 6.9 to 24.1 G Pa with increasing film thickness. Since the testing loads were chosen to keep the depth of indentation to be less than 1/10 of the film thickness, the substrate effect on the hardness values is minimized. Therefore, the increase of hardness is not supposed to be from the increase of substrate effect as the film thickness increases.

In summary, the film hardness is apparently influenced by the film thickness; however, since the packing factor and texture coefficient are also changed with the film thickness, the effective parameters that affect the film hardness are texture coefficient and packing factor. Figure 6 depicts the surface morphology of the specimen SEM test. Comparing Figure 11 with Figure 12, a very smooth surface structure and no columnar structure are observed by Scanning Electron Microscopy (SEM). This may mean that the formed TiN crystal size is small and the columnar morphology is destroyed.

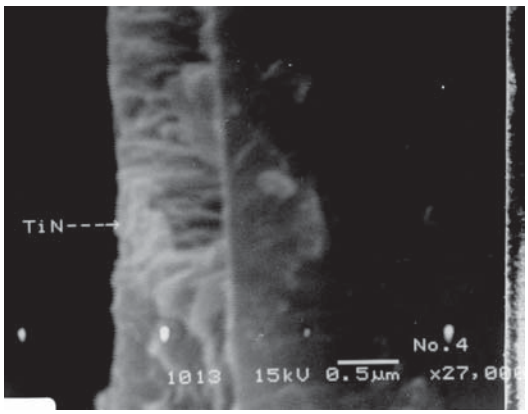

Figure 12 SEM micrograph of the surface of TiN coated stainless stell.

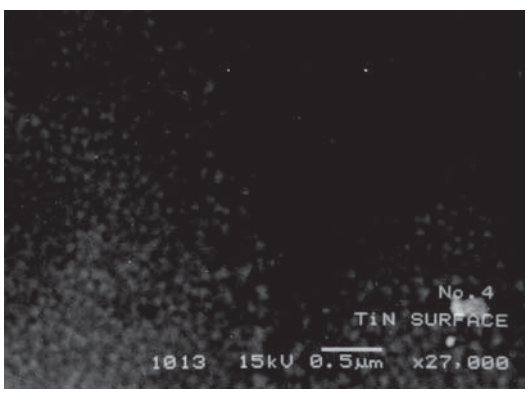

Figure 13 SEM micrograph of the TiN coated stainless stell.

In contrast, Raman spectroscopy is non-destructive and may be performed under ambient conditions. Furthermore, the molecular vibration signatures obtained from a Raman spectrum are very sensitive to chemical structure and bonding, rather than just atomic composition. Previous studies have applied micro-Raman method (Chire, 2003; Valvada, 1996) to probe tribological surfaces where the Raman measurements have been performed using either single-point or line –scan method. The former produces a spectrum representing the average chemical composition over the area that is illuminated (which can be as small as 1mm in diameter) and the latter produces an array of spectra along a line on the surface. In order to produce Raman images, previous methods required laborious raster scanning of the sample. This is also confirmed by the SEM image of an untested dry TiN surface shown in Figure 12 which shows only the presence of TiN. The deposited film has an uniform golden colour. The relative ratio of nitrogen and titanium (N/Ti) is given about 1:10 in film by Raman spectroscopy. Figure 9 shows the spectra of color surface of TiN coated on stainless steel.

ACKNOWLEDGEMENTS

P. Limsuwan wishes to thank the Department of Physics, Faculty of Science, King Mongkut's University of Technology Thonburi and Mahidol University for proving generous grants to make this research possible.

LITERATURE CITED

Badisch E., G.A. Fontalvo, M. Stoiber and C.Mitterer, 2003. Tribological behavior of PACVD TiN coatings in the temperature range up to 500°C. **Surf. Coat.Technol**. 163/164 : 585.

Chire J., Carmalt, Anne Newport, P. Ivan Parkin, P. Mountford, J. Andrew, Sealey and Stuart R. Dubberley, 2003. Syntyesis of TiN thin film from titanium complexes. **J. Mater. Chem**. 13 : 84.

Chou. Wen-Jun., Ge-Ping Yu and J.-Hong Hung, 2002. Mechanical properties of TiN thin film coatings on 304 stainless steel substrate. **Surf.Coat.Technol**. 149 : 7.

Harma H., T. Inoue, S. Nakashima, H. Okumura, Y. Ihasida, S. Yoshida, T. Koizumi, H. Grille and F. Bechsted, 1999. Raman spectrum and phonon modes of AlGsN. **Appl.Phys.Lett.** 74 : 191.

Hoffman D.W., 1998. Titanium nitride coated hardness by PVCD.**Vacuum and Surface**

Anakysis 2 : 183.

Hohl F., S-R. Stok and P. Mayr, 1992. **Surf. Coat.Technol**. 54/55 : 160.

Huang J-H., Y.-P. Tsai and G.-P. Yu, 1999. Effect of processing parameters on the microstructure and mechanical properties of TiN film on stainless steel by HCD ion plating. **Thin.Solid.Film**. 355-356.440.

Karin N. Jallad and Dor. Ben-Amotz, 2002. Raman chemical imaging of tribological nitride coated (TiN, TiAlN) surfaces. **Wear** 252 : 965.

McNeil L., M. Grimsditch and R. French, 1993. TiN films coated on stainless steel. **J.Am.Ceram.Soc.** 76 : 1132.

Richter F., H. Kupfer, H. Giegengack, G. Schaarschmidt, F. Scholze, F. Elsner and G. Hecht. 1996. Fundamental mechanisms of titanium nitride formation by d.c. magnetron sputtering. **Surf. Coat. Technol**. 85 : 61

Vaclav V., 1996, Structure of TiN coatings. **Surf.Coat.Technol**. 80 : 61.

Ye M. Y., O. Matsuda, N. Ohno, M. Takgi, Y. Uesugi and S. Takamura, 1998. Deposition of TiN thin films with strongly ionzed plasmas in high duty AC to kamak discharge. **ECA** 22 : 2769.